

Ferrimagnetism in Fe-rich NbFe₂

T. D. Haynes,¹ I. Maskery,² M. W. Butchers,² J. A. Duffy,² J. W. Taylor,³ S. R. Giblin,³ C. Utfeld,¹ J. Laverock,¹ S. B. Dugdale,¹ Y. Sakurai,⁴ M. Itou,⁴ C. Pfleiderer,⁵ M. Hirschberger,^{5,6} A. Neubauer,⁵ W. Duncan,⁷ and F. M. Grosche⁶

¹*H. H. Wills Physics Laboratory, University of Bristol, Tyndall Avenue, Bristol BS8 1TL, United Kingdom*

²*Department of Physics, University of Warwick, Coventry CV4 7AL, United Kingdom*

³*ISIS Facility, Rutherford Appleton Laboratory, Chilton, Oxfordshire, OX11 0QX, United Kingdom*

⁴*Japan Synchrotron Radiation Research Institute, SPring-8, 1-1-1 Kouto, Sayo, Hyogo 679-5198, Japan*

⁵*Technische Universität München, Physik-Department E21, James-Frank-Strasse, D-85748 Garching, Germany*

⁶*Cavendish Laboratory, University of Cambridge, JJ Thomson Avenue, Cambridge CB3 0HE, United Kingdom*

⁷*Department of Physics, Royal Holloway, University of London, Egham TW20 0EX, United Kingdom*

(Received 16 February 2012; revised manuscript received 15 March 2012; published 30 March 2012)

We report a study of the spin moment in single crystal Nb_(1-y)Fe_(2+y) with $y = 0.015$ using spin-dependent Compton scattering in conjunction with *ab initio* electronic structure calculations. From the experiment, we find that the total spin moment is $0.245 \pm 0.004\mu_B$. Comparison of the measured spin density with theoretical results from linearized muffin-tin orbital calculations determines there to be a *ferrimagnetic* arrangement of Fe moments, with the $2a$ Fe site aligned antiparallel to the bulk moment. There is a small moment on the Nb site, also antiparallel to the net moment. The orbital moment has been determined to be $0.02 \pm 0.02\mu_B$.

DOI: [10.1103/PhysRevB.85.115137](https://doi.org/10.1103/PhysRevB.85.115137)

PACS number(s): 71.20.Lp, 75.50.Bb, 75.10.Lp

I. INTRODUCTION

Nb_(1-y)Fe_(2+y) displays a rich phase diagram at low temperature, with three distinct phases accessible across a narrow compositional range,¹⁻⁶ as depicted in Fig. 1. Iron-rich samples ($y > 0.01$), exhibit remanent magnetization at low temperature, and have therefore been labeled as ferromagnetic. As the iron excess is reduced, this evolves into an ordered state without remanent magnetization, which is usually interpreted as spin density wave order (SDW). The SDW state persists into the niobium-rich compositions, for y up to ~ -0.015 . A second ferromagnetic state emerges in very niobium-rich samples ($y < -0.02$). The threshold of SDW order at $y = -0.015$ may represent a quantum critical point, which is reflected in rather unusual non-Fermi liquid temperature dependencies of the electrical resistivity and of the heat capacity.⁵ These anomalies, observed over a range of compositions about the critical point, suggest the presence of both ferromagnetic and significant antiferromagnetic fluctuations.⁶

The hexagonal C14 Laves structure of NbFe₂, characterized by a double layer of kagome lattice sheets formed by the $6h$ Fe sites, motivated early suggestions that frustration may be behind the quantum criticality (QC) exhibited by this system.⁷ The transport and thermodynamic properties of Nb_(1-y)Fe_(2+y) as a function of its stoichiometry have recently been clarified.⁸ However, the underlying magnetic structure in both the proposed SDW phase and the ferromagnetic phases remains unclear. In the SDW phase standard techniques such as neutron diffraction show no signature of long-range order,⁹ although evidence of such order has been inferred from NMR experiments.^{2,10} It has been proposed that the system may be ordered, but that a long-range modulation is present which has not yet been observed. The lack of magnetic structural and dynamic information means that very little is actually known about the spin density in Nb_(1-y)Fe_(2+y).

Asano and Ishida¹¹ were the first to report the possible magnetic ground states of NbFe₂ through electronic structure calculation. They found a number of different magnetic

orderings with similar energies, of which the lowest energy state proved to be the same antiferromagnetic state as in TiFe₂.¹² Recently there has been a renewed theoretical interest in NbFe₂. Subedi and Singh¹³ reported a comprehensive study of different possible collinear magnetic states, and also investigated the possibility of frustration due to the kagome lattice. They argued that as the antiferromagnetic nearest-neighbor interactions are weak and the electronic structure quite three dimensional, geometric frustration in the $6h$ plane was unlikely to be the main cause of the QC. They suggest that the QC may be a result of a number of nearly degenerate states arising from competition between the $6h$ plane and the $2a$ Fe sites. Contrary to Ref. 11 they found the state with lowest energy to possess a ferrimagnetic ordering of the site moments.

A study by Tompsett *et al.*¹⁴ made the case that nonrigid band effects due to disorder are the cause of the diverse phase diagram of NbFe₂. They also suggested that Fermi surface nesting may be behind some of the non-FL behavior (although they found no peak in the real part of the static susceptibility). They also found a different ground state from Ref. 13, an antiferromagnetic solution which had not previously been considered.¹⁵ More recently Neal *et al.*¹⁶ have published a study on the electronic structure of NbFe₂, finding a ferrimagnetic solution to have the lowest energy. They argued that an unconventional band critical point (uBCP), a special kind of van-Hove singularity, is the source of the critical fluctuations in NbFe₂. Most recently Alam and Johnson¹⁷ were able to treat the effects of disorder accurately by using the coherent potential approximation within the Korringa, Kohn and Rostoker (KKR), and showed that this uBCP crossed the Fermi level at the critical level of Nb excess. While posing different mechanisms for the QC, these studies agree that the energy differences between the possible magnetic ground states are very small, and the question of whether an experimental measurement is able to resolve the true magnetic ground state adopted by Nb_(1-y)Fe_(2+y) remains open.

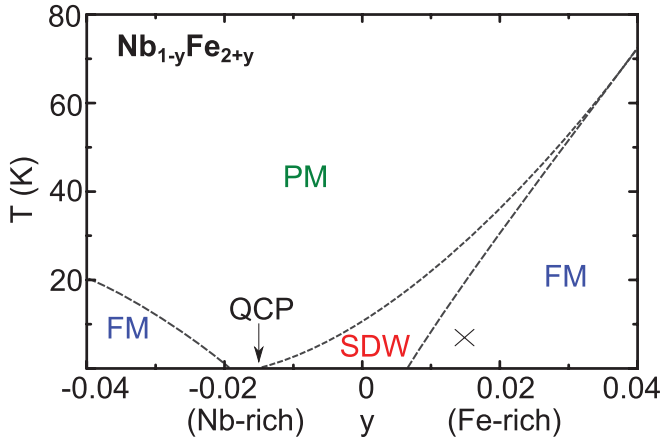


FIG. 1. (Color online) Phase diagram of $\text{Nb}_{1-y}\text{Fe}_{2+y}$, adapted from.⁸ The \times marks the composition and temperature for the experimental measurement reported in this paper.

Determining the magnetic structure of NbFe_2 is central to understanding its behavior, motivating numerous experimental investigations. An NMR study by Yamada and Sakata² was able to resolve weak antiferromagnetic order with a T_N of $\sim 10\text{K}$ for near stoichiometric samples; prior to this NbFe_2 was thought to be paramagnetic.¹⁸ More recently a ferromagnetic component was also observed by Turtelli *et al.* at 4.2K .¹⁹ This evidence of both antiferromagnetic and ferromagnetic fluctuations led to their suggestion that a spin density wave (SDW) state was being exhibited. Samples further from stoichiometry adopt a state with ferromagnetic (or possibly ferrimagnetic) order.²

In this paper, we report the results of spin-dependent Compton scattering measurements on a single crystal of $\text{Nb}_{0.985}\text{Fe}_{2.015}$, believed to possess ferromagnetic ordering at low temperature, with the aim of experimentally determining its true magnetic ground state.

II. EXPERIMENTAL DETAILS

Magnetic Compton scattering is an ideal technique for the study of spin moments.^{20,21} The quantity measured in a Compton scattering experiment, the so-called Compton profile, is defined as a one-dimensional (1D) projection onto the scattering vector of the electron momentum distribution.^{22,23} The spin dependence may then be isolated by either flipping the direction of magnetization within the sample or the photon helicity between parallel and antiparallel with respect to the scattering vector, and computing the difference between these quantities.²⁴ The integrated area of this magnetic Compton profile (MCP) is proportional to the total spin moment per formula unit of the sample.²⁵ Comparison with a reference sample (Ni) in which the spin moment is well known allows the determination of the spin moment of the sample. The orbital moment is not observed,²⁶ allowing its value to be determined by comparing the Compton measurement with a bulk magnetization measurement. The incoherent nature of Compton scattering means that all local and itinerant contributions to the spin moment are observed. Also, the high x-ray energies used in the experiments, typically well above 100keV , mean that the bulk electronic structure is measured.

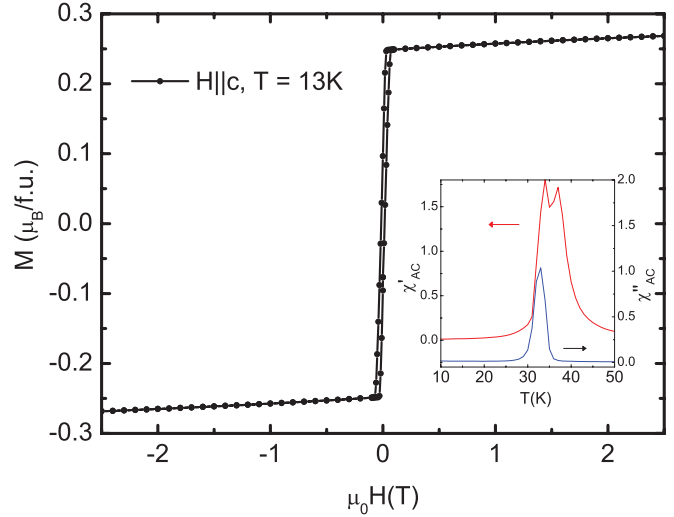


FIG. 2. (Color online) Bulk dc magnetization of the $\text{Nb}_{0.985}\text{Fe}_{2.015}$ single crystal at 13K . The inset shows the zero-field ac susceptibility.

The spin-polarized Compton profile presented here was measured on beamline BL08W at the SPring-8 synchrotron. The measurements were made in an applied magnetic field of 2.5T , using a superconducting solenoid, and which was reversed every 60s in order to measure the difference profile. An incident energy of 175keV was used. The energy spectrum of the scattered flux was measured using a 10-element Ge detector at a mean scattering angle of 173° . The momentum resolution of the magnetic Compton spectrometer, taken as the full width at half maximum (FWHM) of the instrument response function, was 0.45a.u. of momentum (where $1\text{a.u.} = 1.99 \times 10^{-24}\text{kg m s}^{-1}$). The data were corrected for energy-dependent detector efficiency, sample absorption, and the relativistic scattering cross section. The profiles were then corrected for multiple scattering using the technique described by Felsteiner.²⁷

Our $\text{Nb}_{0.985}\text{Fe}_{2.015}$ single crystal was grown using the floating zone method in a UHV compatible four-mirror optical image furnace,²⁸ which is capable of heating samples to 2200°C , and which may be evacuated to avoid oxidation. Seed and feed rods were prepared at Royal Holloway, University of London from high purity niobium and iron, and which were then counter-rotated during the floating zone growing process. Rectangular samples of size $3 \times 3 \times 1\text{mm}$ were cut and aligned to have the hexagonal c axis perpendicular to the sample face. Both x-ray and neutron scattering confirmed that the samples were high quality single crystals. Neutron depolarization along with ac susceptibility measurements revealed well-defined homogeneous magnetic phase transitions, with $T_C = \sim 33\text{K}$ and $T^* = \sim 37\text{K}$. dc magnetization measurements revealed a low temperature saturation moment equal to $0.27 \pm 0.02\mu_B$ per formula unit. The magnetic susceptibility data are shown in Fig. 2.

III. ELECTRONIC STRUCTURE CALCULATIONS

Understanding the distribution of magnetic electrons observed in a MCP may be aided by complementary electronic structure calculations. Computing the equivalent electron

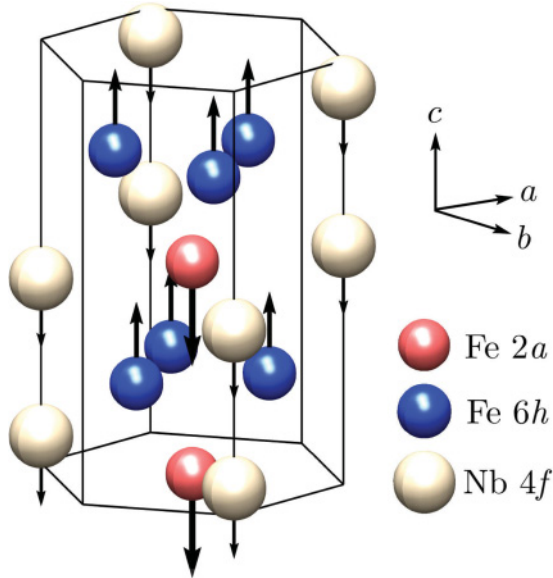


FIG. 3. (Color online) C14 Laves phase of NbFe₂ in the ferrimagnetic state predicted by our LMTO calculation. The arrows on the atomic sites indicate the relative sizes and directions of the respective moments.

momentum density (EMD) from an *ab initio* electronic structure calculation allows the underlying magnetic state observed in the measurement to be determined.

The electronic structure of NbFe₂ was computed using the linear muffin-tin orbital (LMTO) method within the atomic sphere approximation (ASA) with combined correction terms,²⁹ using the local spin density approximation (LSDA) to the exchange correlation functional.³⁰ The LMTO method expresses the ground-state electronic structure in terms of atomiclike muffin-tin orbitals. In order to compute the EMD measured in a Compton scattering experiment these orbitals are expanded onto plane waves before Fourier transforming to momentum space. To obtain the Compton profile, this three-dimensional (3D) EMD is then integrated down the directions orthogonal to the experimental scattering vector. In order to compute the magnetic Compton profile (MCP), the EMDs for the spin-up and spin-down electrons are computed separately, the magnetic EMD being the difference between these two quantities.

The hexagonal C14 Laves phase of NbFe₂ has two inequivalent Fe sites (2*a* and 6*h*), and one Nb site (4*f*), as indicated in Fig. 3. The calculations were converged on 624 *k* points within the irreducible Brillouin zone, using the experimental lattice constant of $a = 4.838 \text{ \AA}$, with $c/a = 1.63$. The effects of doping were incorporated using the virtual crystal approximation (VCA). Our paramagnetic band structure for the stoichiometric compound was found to be in excellent agreement with that of Ref. 13.

We found the lowest energy state to be ferrimagnetic, similar to that found in,¹³ with the same orientation of site moments, albeit with slightly different magnitudes. In particular we find a larger antiparallel moment on the Nb 4*f* site, possibly due to the different partitioning of space in the ASA scheme. A ferromagnetic state with both Fe sites aligned was also stabilized (though it was found to be metastable with

TABLE I. Details of the different sizes and orientations of the ferrimagnetic and ferromagnetic magnetic moments of NbFe₂ in the ferro- and ferrimagnetic states.

Site	Ferri	Ferro
Fe 2 <i>a</i> (μ_B per site)	-0.997	0.222
Fe 6 <i>h</i> (μ_B per site)	0.711	1.29
Nb 4 <i>f</i> (μ_B per site)	-0.161	-0.233
Total (μ_B per f.u.)	0.407	1.83

respect to the ferrimagnetic solution). The sizes of the moments comprising the two states are summarized in Table I.

Our approach was to reproduce the various possible states which have already been investigated theoretically.^{13,14,16} By computing the EMD corresponding to each magnetic state we were able to directly compare to the MCP measured in the experiment and see which are compatible with our measurement. Nb_(1-y)Fe_(2+y) with $y = 0.015$ is known to possess a net magnetic spin moment,¹⁰ and therefore only the ferrimagnetic and ferromagnetic states were considered as candidates for the electronic structure of our sample.

The MCPs produced from the ferrimagnetic and ferromagnetic states are shown in Fig. 4. It is possible to decompose the different contributions to the MCP from each atomic site, along with an interference term between sites. This enables one to determine to which components of the electronic structure the measurement is sensitive. For both states the increase in real space delocalization of the Nb 4*d* electrons relative to the Fe 3*d* electronic states is observable as an increase of the localization of Nb 4*d* contribution in momentum space.

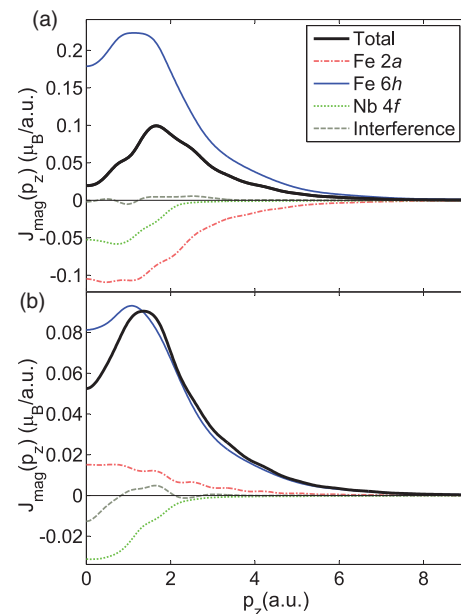


FIG. 4. (Color online) MCPs produced from the LMTO calculation for (a) the ferrimagnetic and (b) the ferromagnetic states of NbFe₂ with the scattering vector along the *c* axis. The different contributions to the MCPs have been resolved onto each inequivalent atomic site, and also the interference term between sites.

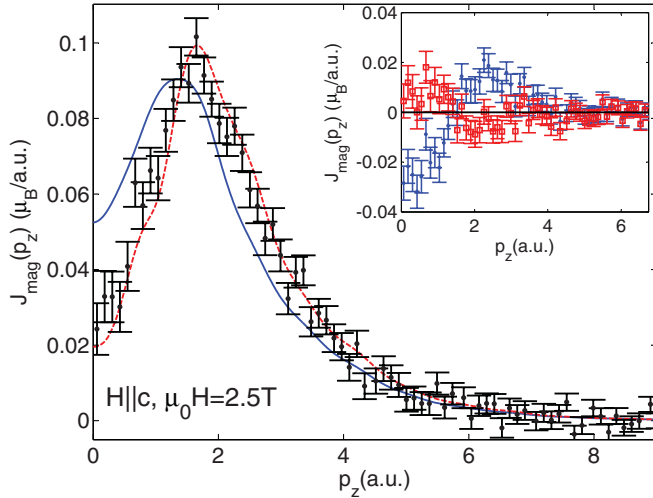


FIG. 5. (Color online) Experimental $\text{Nb}_{0.985}\text{Fe}_{2.015}$ magnetic spin momentum density (black points) projected along the [0001] crystal direction, plotted together with LMTO ferrimagnetic calculation (red dashed line) and ferromagnetic calculation (blue solid line). Both the calculated LMTO profiles have been normalized to the same total spin moment (area). The inset shows difference plots for the experimental data minus each theoretical profile, again with the ferrimagnetic (ferromagnetic) case plotted as red squares (blue points).

IV. RESULTS

The spin moment of the sample, determined from the area under the MCP, was found to be $0.245 \pm 0.004 \mu_B$. Comparing this with the dc susceptibility measurement shown in Fig. 2 indicates the orbital moment of our sample to be $0.02 \pm 0.02 \mu_B$. The MCP was measured along the c axis of the crystal, as it had been determined that the contrast between the possible DFT magnetic states was greatest when the EMDs were viewed down this direction. The magnetic field was applied parallel to the scattering vector of the x rays and thus along the c axis of the crystal. The measured MCP is shown in Fig. 5, plotted with the LMTO prediction for a ferromagnetic and a ferrimagnetic state.

Both calculations substantially overestimate the saturation spin moment, as they fail to fully describe spin fluctuations.³¹ Our analysis therefore considers just the *shape* of the profiles, not their *area*. The agreement between the ferrimagnetic solution and the measured profile is far superior to that of the ferromagnetic state. In terms of the shapes of the two calculated profiles, the main difference occurs at momentum values below ≈ 2 a.u., with both profiles exhibiting similar Fe 3d character at higher momentum. We note that the level of discrepancy at low momentum in the ferromagnetic model could be reduced if

the amount of itinerant moment has been underestimated. The levels of agreement between the two different models shown and the experimental data were assessed through a χ^2 test in which the ferromagnetic state yielded a reduced χ^2 of 4.2 compared to just 1.3 for the ferrimagnetic state. This strongly suggests that the ferrimagnetic solution originally predicted by Subedi and Singh is the ground state of NbFe_2 for samples with an iron excess of 0.015. Furthermore, the agreement between the ferrimagnetic calculation and experiment requires that the ratios of the predicted site moments obtained from calculation are largely accurate; the renormalization of the total moment caused by spin fluctuations appears not to significantly alter the relative sizes of each site moment. This can be seen from Fig. 4(a), in which the shape of the profile below ~ 1.7 a.u. is sensitive to the relative contributions of all the site moments. This implies that the renormalized site moments observed in the experimental MCP are of the order $0.4 \mu_B$ for the Fe $6h$ site, $-0.6 \mu_B$ for the Fe $2a$ site, and $-0.1 \mu_B$ for the Nb $4f$ site. Our results find the magnetic structure of $\text{Nb}_{0.985}\text{Fe}_{2.015}$ to be consistent with that predicted by electronic structure calculations, albeit renormalized by a factor of 0.6.

In summary, we present the spin-dependent momentum density of Fe-rich NbFe_2 , the interpretation of which has been facilitated by electronic structure calculations. We demonstrate that the shape of the experimental profile is consistent with a ferrimagnetic ground state in which the two inequivalent Fe sites order antiparallel to one another. Our calculations clearly show that a ferromagnetic ground state is unable to account for the measured spin density. Therefore our measurement resolves the magnetic structure of the state previously supposed to be ferromagnetic on the iron-rich side of the $\text{Nb}_{(1-y)}\text{Fe}_{(2+y)}$ phase diagram, the state from which QC emerges as the iron content is reduced. Furthermore these results highlight the interesting observation that incoherent Compton scattering can be used to unambiguously resolve, from a highly degenerate manifold, the magnetic ground state and structure. This suggests that it may be possible to measure the magnetic structure of NbFe_2 over a wide range of stoichiometry.

ACKNOWLEDGMENTS

We acknowledge the financial support of the United Kingdom Engineering and Physical Sciences Research Council, via Grants No. EP/H009140/1 and No. EP/F021518/1, and that of the German Science Foundation (DFG-FOR960). This experiment was performed with the approval of the Japan Synchrotron Radiation Research Institute (JASRI) (Proposal No. 2009A1454).

¹M. Shiga and Y. Nakamura, *J. Phys. Soc. Jpn.* **56**, 4040 (1987).

²Y. Yamada and A. Sakata, *J. Phys. Soc. Jpn.* **57**, 46 (1988).

³M. R. Crook and R. Cywinski, *J. Magn. Magn. Mater.* **140**, 71 (1995).

⁴W. J. Duncan, O. P. Welzel, D. Moroni-Klementowicz, C. Albrecht, P. G. Niklowitz, D. Grüner, M. Brando, A. Neubauer, C. Pfleiderer, N. Kikugawa, A. P. Mackenzie, and F. M. Grosche, *Phys. Status Solidi B* **247**, 544 (2010).

⁵M. Brando, W. J. Duncan, D. Moroni-Klementowicz, C. Albrecht, D. Grüner, R. Ballou, and F. M. Grosche, *Phys. Rev. Lett.* **101**, 026401 (2008).

⁶D. Moroni-Klementowicz, R. Burrell, D. Fort, and M. Grosche, *Physica B* **359-361**, 80 (2005).

⁷M. R. Crook and R. Cywinski, *Hyperfine Interact.* **85**, 203 (1994).

⁸D. Moroni-Klementowicz, M. Brando, C. Albrecht, W. J. Duncan, F. M. Grosche, D. Grüner, and G. Kreiner, *Phys. Rev. B* **79**, 224410 (2009).

- ⁹M. Brando, D. Moroni-Klementowicz, C. Albrecht, and F. M. Grosche, *Physica B* **378-380**, 111 (2006).
- ¹⁰Y. Yamada *et al.*, *J. Phys. Soc. Jpn.* **59**, 2976 (1990).
- ¹¹S. Asano and S. Ishida, *J. Phys.: Condens. Matter* **1**, 8501 (1989).
- ¹²P. J. Brown, J. Deportes, and B. Ouladdiaf, *J. Phys.: Condens. Matter* **4**, 10015 (1992).
- ¹³A. Subedi and D. J. Singh, *Phys. Rev. B* **81**, 024422 (2010).
- ¹⁴D. A. Tompsett, R. J. Needs, F. M. Grosche, and G. G. Lonzarich, *Phys. Rev. B* **82**, 155137 (2010).
- ¹⁵Note: The Tompsett group also used a different exchange correlation functional from Subedi and Singh (GGA rather than LSDA), which may explain the different state energies found.
- ¹⁶B. P. Neal, E. R. Ylvisaker, and W. E. Pickett, *Phys. Rev. B* **84**, 085133 (2011).
- ¹⁷A. Alam and D. D. Johnson, *Phys. Rev. Lett.* **107**, 206401 (2011).
- ¹⁸S. Ishida, S. Asano, and J. Ishida, *J. Phys. Soc. Jpn.* **54**, 3925 (1985).
- ¹⁹R. Sato Turtelli *et al.*, *J. Magn. Magn. Mater.* **316**, 492 (2007).
- ²⁰J. A. Duffy, S. B. Dugdale, J. E. McCarthy, M. A. Alam, M. J. Cooper, S. B. Palmer, and T. Jarlborg, *Phys. Rev. B* **61**, 14331 (2000).
- ²¹J. E. McCarthy, J. A. Duffy, C. Detlefs, M. J. Cooper, and P. C. Canfield, *Phys. Rev. B* **62**, R6073 (2000).
- ²²P. M. Platzman and N. Tzoar, *Phys. Rev.* **2**, 3556 (1970).
- ²³P. Holm, *Phys. Rev. A* **37**, 3706 (1988).
- ²⁴F. Bell, J. Felsteiner, and L. P. Pitaevskii, *Phys. Rev. A* **53**, R1213 (1996).
- ²⁵M. A. G. Dixon, J. A. Duffy, M. J. Cooper, J. E. McCarthy, S. Gardelis, D. N. Timms, S. B. Dugdale, and T. Jarlborg, *J. Phys.: Condens. Matter* **10**, 2759 (1998).
- ²⁶P. Carra, M. Fabrizio, G. Santoro, and B. T. Thole, *Phys. Rev. B* **53**, R5994 (1996).
- ²⁷J. Felsteiner, P. Pattison, and M. J. Cooper, *Philos. Mag.* **30**, 537 (1974).
- ²⁸A. Neubauer, J. Boeuf, A. Bauer, B. Russ, H. V. Löhneysen, and C. Pfleiderer, *Rev. Sci. Instrum.* **82**, 013902 (2011).
- ²⁹B. Barbiellini, S. B. Dugdale, and T. Jarlborg, *Comput. Mater. Sci.* **28**, 287 (2003).
- ³⁰O. Gunnarsson and B. I. Lundqvist, *Phys. Rev. B* **13**, 10 (1976).
- ³¹A. Aguayo, I. I. Mazin, and D. J. Singh, *Phys. Rev. Lett.* **92**, 147201 (2004).